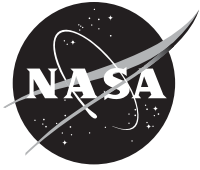


NASA/TM—2014-218292



Glenn Goddard TDRSS Waveform 1.1.3 On-Orbit Performance Report

David T. Chelmins
Glenn Research Center, Cleveland, Ohio

NASA STI Program . . . in Profile

Since its founding, NASA has been dedicated to the advancement of aeronautics and space science. The NASA Scientific and Technical Information (STI) program plays a key part in helping NASA maintain this important role.

The NASA STI Program operates under the auspices of the Agency Chief Information Officer. It collects, organizes, provides for archiving, and disseminates NASA's STI. The NASA STI program provides access to the NASA Aeronautics and Space Database and its public interface, the NASA Technical Reports Server, thus providing one of the largest collections of aeronautical and space science STI in the world. Results are published in both non-NASA channels and by NASA in the NASA STI Report Series, which includes the following report types:

- **TECHNICAL PUBLICATION.** Reports of completed research or a major significant phase of research that present the results of NASA programs and include extensive data or theoretical analysis. Includes compilations of significant scientific and technical data and information deemed to be of continuing reference value. NASA counterpart of peer-reviewed formal professional papers but has less stringent limitations on manuscript length and extent of graphic presentations.
- **TECHNICAL MEMORANDUM.** Scientific and technical findings that are preliminary or of specialized interest, e.g., quick release reports, working papers, and bibliographies that contain minimal annotation. Does not contain extensive analysis.
- **CONTRACTOR REPORT.** Scientific and technical findings by NASA-sponsored contractors and grantees.

- **CONFERENCE PUBLICATION.** Collected papers from scientific and technical conferences, symposia, seminars, or other meetings sponsored or cosponsored by NASA.
- **SPECIAL PUBLICATION.** Scientific, technical, or historical information from NASA programs, projects, and missions, often concerned with subjects having substantial public interest.
- **TECHNICAL TRANSLATION.** English-language translations of foreign scientific and technical material pertinent to NASA's mission.

Specialized services also include creating custom thesauri, building customized databases, organizing and publishing research results.

For more information about the NASA STI program, see the following:

- Access the NASA STI program home page at <http://www.sti.nasa.gov>
- E-mail your question to help@sti.nasa.gov
- Fax your question to the NASA STI Information Desk at 443-757-5803
- Phone the NASA STI Information Desk at 443-757-5802
- Write to:
STI Information Desk
NASA Center for AeroSpace Information
7115 Standard Drive
Hanover, MD 21076-1320

NASA/TM—2014-218292



Glenn Goddard TDRSS Waveform 1.1.3 On-Orbit Performance Report

David T. Chelmins
Glenn Research Center, Cleveland, Ohio

National Aeronautics and
Space Administration

Glenn Research Center
Cleveland, Ohio 44135

May 2014

Trade names and trademarks are used in this report for identification only. Their usage does not constitute an official endorsement, either expressed or implied, by the National Aeronautics and Space Administration.

Level of Review: This material has been technically reviewed by technical management.

Available from

NASA Center for Aerospace Information
7115 Standard Drive
Hanover, MD 21076-1320

National Technical Information Service
5301 Shawnee Road
Alexandria, VA 22312

Available electronically at <http://www.sti.nasa.gov>

Glenn Goddard TDRSS Waveform 1.1.3 On-Orbit Performance Report

David T. Chelmins
National Aeronautics and Space Administration
Glenn Research Center
Cleveland, Ohio 44135

Background and Introduction

The objective of the Space Communications and Navigation (SCaN) Testbed is to study the development, testing, and operation of software defined radios and their associated applications in the operational space environment to reduce cost and risk for future space missions. The SCaN Testbed was launched on July 20, 2012 to the International Space Station (ISS) on a Japanese H-II Transfer Vehicle (JAXA HTV3), and transferred and installed via Extravehicular Robotics (EVR) on the ExPRESS Logistics Carrier-3 (ELC3) in the inboard, Ram-facing, Zenith-facing payload location on an exterior truss of the ISS (Figure 1).

SCaN Testbed contains three software-defined radios, which provide data communications capabilities that can be reconfigured on-demand by software changes. The software that defines the communications behavior is referred to as a “waveform”. The simplest SDR consists of an analog-to-digital converter (ADC), a digital-to-analog converter (DAC), a diplexer, and an antenna. The waveform defines the digital signals that are sent to and received from the ADC and DAC, respectively.

The Jet Propulsion Laboratory (JPL) software-defined radio (SDR), shown in Figure 2, is one of the SDRs in the testbed that supports full-duplex communications at S-band and simplex receive operation at L-band frequencies. The S-band capabilities of the radio have been tested with NASA’s Tracking and Data Relay Satellite System (TDRSS) network of geosynchronous satellites. An engineering model (EM) of the JPL SDR remains at the NASA Glenn Research Center (GRC) on the ground, installed into the SCaN Testbed Ground Integration Unit (GIU) for development and testing.

The Glenn Goddard TDRSS (GGT) waveform, version 1.1.3, was installed on the JPL SDR prior to launch to ISS. This waveform is compliant with the capabilities of TDRSS and allows the radio to support full-duplex communication with a Tracking and Data Relay Satellite (TDRS). A block diagram of the waveform functionality is shown in Figure 3. The waveform operates using binary phase shift keying (BPSK), and it is compliant with the Space Telecommunications Radio System (STRS) architecture standard.

An extensive set of communications testing was performed with the GGT waveform prior to launch of SCaN Testbed. The GGT Waveform Performance Databook (SCaN Testbed project document GRC-CONN-DBK-0924) documents the waveform performance on the ground. This set of performance data will be used as a baseline for evaluating on-orbit performance.

This report covers the results of on-orbit performance testing completed using the waveform configurations in Table 1 over TDRSS. Testing was completed between January 2013 and April 2013, with operations coordinated from the Telescience Center (TSC) at the GRC, shown in Figure 4. Some of the tests helped debug problems with the end-to-end data paths and ground support systems that are part of the SCaN Testbed.



Figure 1.—SCaN Testbed Installed on ISS

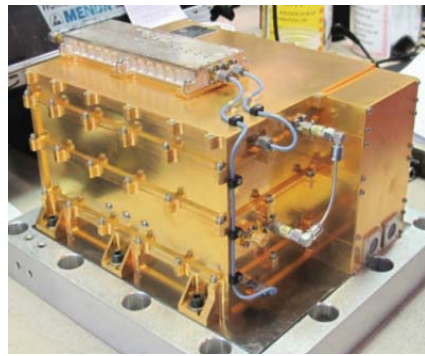


Figure 2.—JPL Software Defined Radio

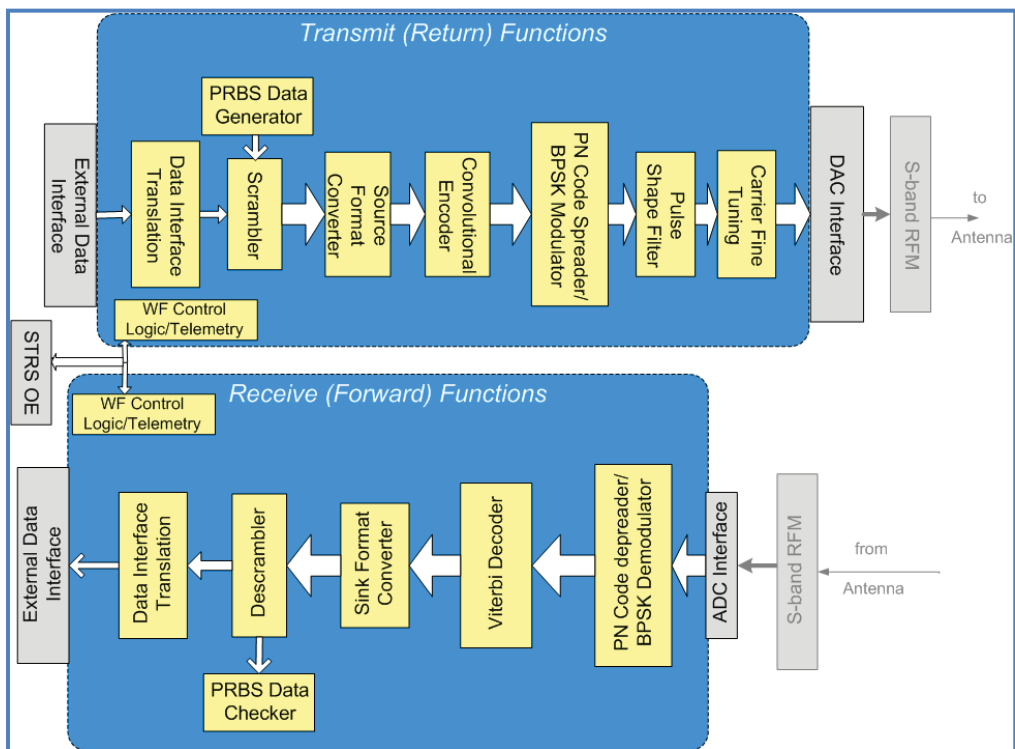


Figure 3.—GGT Waveform Functional Diagram



Figure 4.—SCaN Testbed Operations at the GRC TSC (NASA C-2012-650)

TABLE 1.—GGT MODES OF OPERATION

Mode	Description	TDRSS service	Data rate Tx/Rx, kbps	Symbol rate Tx/Rx, kSps	PN modulation	Coded and scrambled
A	VLDR Test Mode (Data Group 1, Mode 2)	MA	24 / 18	24 / 18	On	Off
B	VLDR Operational Mode (Data Group 1, Mode 2)	MA	24 / 18	48 / 36	On	On
C	VLDR Test Mode (Data Group 1, Mode 2)	SA	24 / 18	24 / 18	On	Off
D	VLDR Operational Mode (Data Group 1, Mode 2)	SA	24 / 18	48 / 36	On	On
E	LDR Test Mode (Data Group 2)	SA	192 / 155	192 / 155	Off	Off
F	LDR Operational Mode (Data Group 2)	SA	192 / 155	384 / 310	Off	On
G	MDR Test Mode (Data Group 2)	SA	769 / 769	769 / 769	Off	Off
H	MDR Operational Mode (Data Group 2)	SA	769 / 769	1539 / 1539	Off	On

Although the GGT waveform is completely configurable, it also provides several standard configurations, known as “modes”. Each mode, referenced by a letter, defines the full-duplex behavior of the waveform (e.g., frequency, data rate, error correction). A full listing of the waveform modes tested on-orbit is shown in Table 1. Each mode is classified as very low data rate (VLDR), low data rate (LDR), or medium data rate (MDR). TDRSS provides either single access (SA) or multiple access (MA) services (refer to the Space Network User’s Guide, 450-SNUG, published by the Goddard Space Flight Center). The waveform is capable of spread-spectrum operation by modulating with a pseudo-noise (PN) code. Forward error correction (coding) is implemented using a rate-1/2 convolutional code.

The SA and MA services have assigned frequencies. SCA-N Testbed has a 2216.5 MHz return link and a 2041.027 MHz forward link when using the SA service. The MA service uses a 2287.5 MHz return link and a 2106.5 MHz forward link. These frequencies are negotiated through the NASA spectrum management office.

The next several sections will outline the testing conducted with GGT 1.1.3 and make relevant comparisons to testing completed on the ground using the waveform. The objective of this report is to provide a performance baseline for future users of the JPL SDR. The report will also provide a gauge for the radio frequency (RF) link prediction accuracy.

GGT Waveform Tests Executed On-Orbit

Table 2 shows a list of the test events that involved the GGT waveform version 1.1.3.

TABLE 2.—GGT 1.1.3 ON-ORBIT TESTS

Date	Day of year	SN event	Waveform mode	RF link direction	Forward link result	Return link result
01/29/2013	29	2	D	Receive Only	(1)	N/A
01/29/2013	29	3-1	A	Receive Only	(1)	N/A
01/29/2013	29	3-2	A	Receive Only	✓	N/A
01/29/2013	29	4-1	A	Receive Only	✓	N/A
01/29/2013	29	4-2	B	Receive Only	✓	N/A
02/05/2013	36	2	A	Full Duplex	(2)	✓
02/05/2013	36	4	C	Full Duplex	(1)	✓
02/05/2013	36	5	C	Full Duplex	(2)	✓
02/06/2013	37	1	E	Full Duplex	(2)	✓
02/06/2013	37	2	G	Full Duplex	(3)	✓
02/06/2013	37	3	A	Full Duplex	✓	✓
02/06/2013	37	4	C	Full Duplex	✓	✓
02/06/2013	37	5	C	Full Duplex	✓	✓
02/10/2013	41	1	F	Full Duplex	(1)	✓
02/10/2013	41	2	A	Full Duplex	✓	✓
02/10/2013	41	3	A	Full Duplex	✓	✓
02/10/2013	41	4-1	E	Full Duplex	✓	✓
02/10/2013	41	4-2	F	Full Duplex	(1)	(1)
02/10/2013	41	5	C	Full Duplex	✓	✓
02/12/2013	43	1	H	Full Duplex	(1)	✓
02/13/2013	44	1	B	Receive Only	✓	N/A
02/13/2013	44	2	D	Full Duplex	✓	✓
02/13/2013	44	3	D	Full Duplex	✓	(2)
04/01/2013	91	1	D	Full Duplex	✓	✓
04/01/2013	91	2	D	Full Duplex	✓	✓
04/01/2013	91	3	D	Full Duplex	✓	✓
04/02/2013	92	1	F	Full Duplex	✓	✓
04/02/2013	92	2	F	Full Duplex	✓	✓
04/04/2013	94	1	G	Full Duplex	✓	✓
04/04/2013	94	2	G	Full Duplex	✓	✓
04/16/2013	106	1	H	Full Duplex	✓	✓
04/16/2013	106	2	H	Full Duplex	✓	✓

- ✓ – Test passed: the link behavior was consistent with expectations
- (1) – Test failed: no data was received on the link
- (2) – Test failed: bit errors were introduced by the ground system
- (3) – Test failed: the waveform was unable to lock on the RF signal

Several of the early events in Table 2 experienced problems with the data path. Most of these issues were resolved between Julian day of year (DOY) 44 and DOY 91. Nevertheless, even events affected by data issues provide useful information about the RF link.

Bit Error Rate Performance

The bit error rate (BER) is the primary metric used to evaluate the performance of the GGT waveform. BER traditionally is evaluated in terms of a corresponding energy-per-bit to noise density (Eb/N0) ratio. The BER of a test, or the number of incorrect bits received divided by the total number of bits received, is actually an indicator of an underlying binomial statistical distribution. This distribution can be estimated by a Poisson distribution with the equation:

$$-n \cdot p = \ln(1 - CL) - \ln\left(\sum_{k=0}^N \left(\frac{(n \cdot p)^k}{k!}\right)\right)$$

where n is the total number of bits received, p is the bit error rate, CL is the confidence level, and N is the total number of error bits. In order to establish the true BER of the system, an infinite amount of bits would need to be received. The equation above provides a statistical glimpse at the true BER. A common interpretation is that for a given test where N errors were received out of n bits, the underlying bit error rate is p or better with $CL\%$ confidence.

In this report, to save computation time, the BER performance is calculated to a 95 percent confidence level using a Monte Carlo simulation. This is performed using the “berconfint” function in the MATLAB communications toolbox. The result is a range of BERs, with 95% confidence that the true BER is within that range.

Just as there is uncertainty in the BER statistical distribution, there is also uncertainty in the Eb/N0. On-orbit tests are conducted over real links, which have changing path lengths, noise floors, estimated gains and power levels, and other losses. There is a tradeoff between time to collect sufficient bits for BER certainty and time to evaluate a single Eb/N0 with high certainty.

In this report, Eb/N0 is determined from the link prediction. Since Eb/N0 varies over time, a corresponding Eb/N0 range is also provided for each BER measurement. In general, the total variance will be approximately ± 0.5 dB. The ground testing Eb/N0 will not vary, since the power level and noise floor were held relatively steady during BER testing.

BER is also temperature-dependent. The noise figure of the radio’s RF components will vary over temperature. In the JPL radio, the Radio Frequency Module (RFM) contains a temperature sensor which is used to plot noise figure (Figure 5). For more information on the data behind Figure 5, refer to SCA_N Testbed document GRC-CONN-ANA-0854.

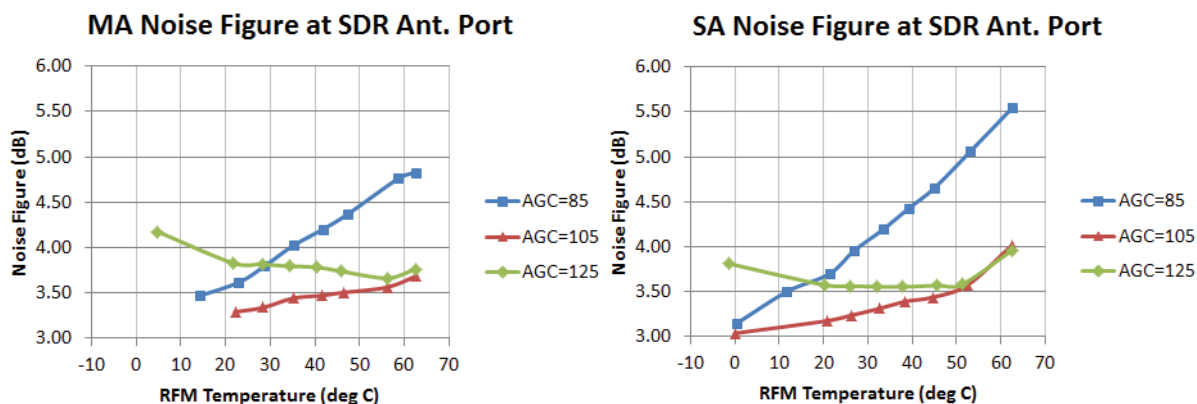


Figure 5.—JPL SDR Noise Figure

Forward Link Bit Error Rate Performance for Uncoded Modes

The GGT 1.1.3 waveform release has a software bug which causes a “flaring” effect in the BER curve. The bug is due to a FPGA register that overflows at high power levels, causing the waveform bit synchronization to see spurious bit flips. On a positive note, the flare makes BER characterization much easier because a characteristic error rate can be established over a wide range of E_b/N_0 values. If the waveform performed closer to theoretical BPSK, many times there would be 0 bit errors over the limited duration of the test RF links.

All BER curves for the GGT uncoded modes (i.e., A, C, E, G) are shown in Figure 6. The *theory* line shows the ideal BPSK modulation performance, the *baseline* line shows the waveform performance measured during ground testing prior to launch, and the *observed* boxes show the waveform performance measured on-orbit. The *baseline* contains vertical lines which show the BER confidence at the measured E_b/N_0 points.

The *observed* boxes each represent a BER point; however they also show the uncertainty in the measurement E_b/N_0 (since the E_b/N_0 was changing while the measurement was taken) and the uncertainty in the BER (since the pass time limits the number of bits that can be collected). The horizontal size of the box represents E_b/N_0 uncertainty, and the vertical size of the box represents BER uncertainty. Note that as the BER becomes worse, the BER becomes more certain since enough bits can be collected to establish that BER.

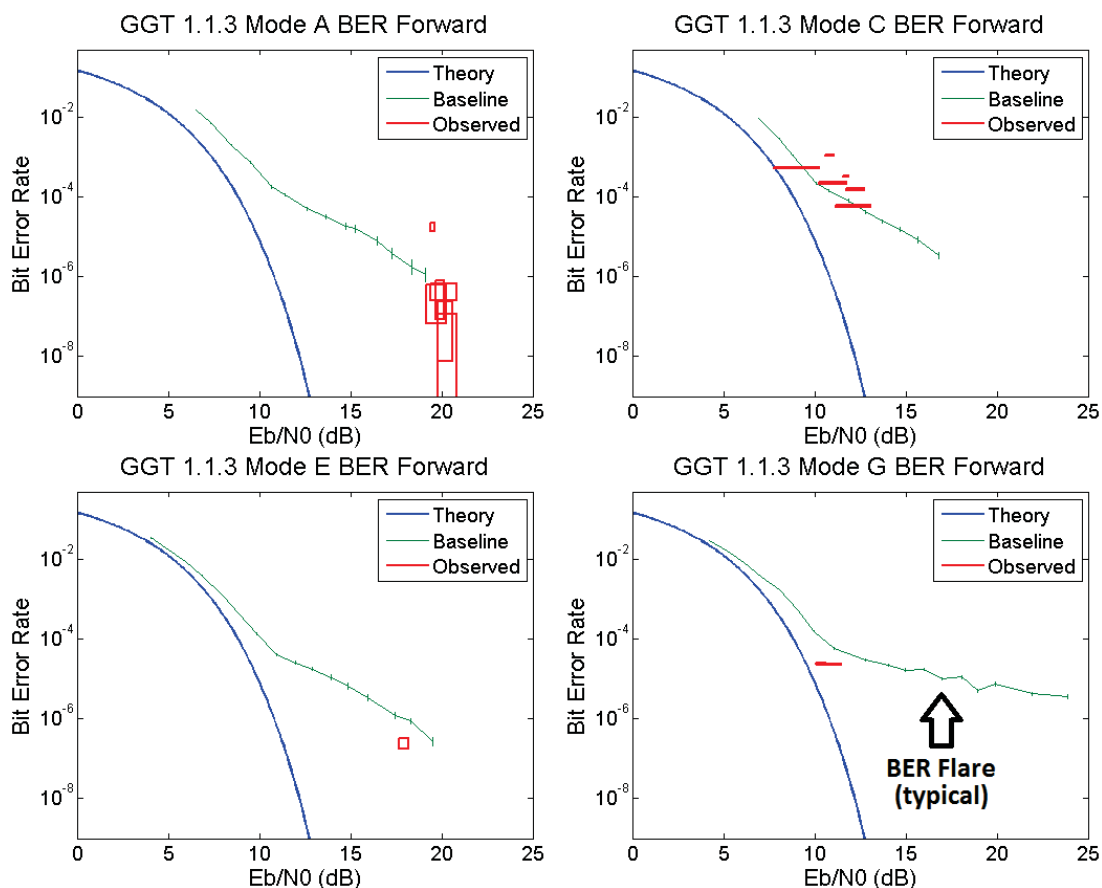


Figure 6.—GGT 1.1.3 Uncoded Forward Link BER Performance

In some cases, the *observed* box extends downwards, outside of the graph. This means that there were 0 errors observed during the duration of the RF link. Statistically, the bit error rate has an upper limit (i.e., the BER is known to be better than some threshold based on the number of bits received). However, the lower limit is unknown. The link could have a BER of 10^{-10} or a BER of 10^{-100} and it would have performed the same during the duration of the test.

Considering the performance in Figure 6, modes A and C generally match the ground baseline while modes E and G perform better than baseline by about 2 dB. The performance improvement could be attributable to at least two factors: 1) noise floor reductions due to lower operating temperatures, and/or 2) incorrect Eb/N0 estimation.

It is unlikely that the waveform performance has improved significantly on-orbit. The RFM temperature during on-orbit testing is generally around 15 to 20 °C, versus 35 to 40 °C during ground testing. Referencing GRC-CONN-ANA-0854, this temperature change could lower the radio noise figure by 0.5 to 1.0 dB at the automatic gain control (AGC) setting of 85, which is the operating point where the noise power saturates the AGC algorithm.

Incorrect Eb/N0 estimation could be due to a number of sources. The Eb/N0 values used for the plots are based on a prediction which takes into account the transmitter power, receiver gain and RF path loss, and antenna patterns and pointing. The TDRS could be transmitting higher power than expected; in many cases, the received power has been 2 to 3 dB above the advertised capability. The Space Network User's Guide (SNUG), which specifies TDRS characteristics, generally contains worst-case numbers that are intended for operational capability instead of calibrated measurements. Additionally, the SCaN Testbed antenna patterns are not precisely known in the International Space Station (ISS) RF environment. The patterns have been characterized on-orbit using the General Dynamics radio (also part of SCaN Testbed), but ultimately this leads to a catch-22 condition where the system under test is being used to establish a reference baseline.

In general, however, the uncoded forward link performance shows that the link can be predicted within 2 to 3 dB accuracy.

Forward Link Bit Error Rate Performance for Coded Modes

The GGT 1.1.3 waveform implements Viterbi decoding for modes B, D, F, and H. In general, a coded waveform mode allows a better BER than an uncoded waveform mode for all Eb/N0s. However, the BER curve becomes steep and more difficult to test. In many cases, the waveform will have a very fine line between not being able to achieve bit synchronization and operating without observed errors. This makes both ground testing and on-orbit testing more challenging.

Coded forward link performance is shown in Figure 7. Testing for modes B, D, and F was completed without any observed errors during the (~40-min) duration of the test. Given the steep BER curves, it would be difficult to manipulate the on-orbit power to match a point on any of the ground/baseline curves. Both tests conducted in mode H produced a BER that was consistent with ground test results, within 1 to 2 dB. This loosely supports the claim that the forward link Eb/N0 is estimated correctly to within 2 dB.

Using GGT 1.1.3, it is possible to receive data without bit errors during a 40 min pass at rates up to 155346 bits per second (bps). Even in mode H (769450 bps), the BER is a low 10^{-7} for tests conducted with TDRSS.

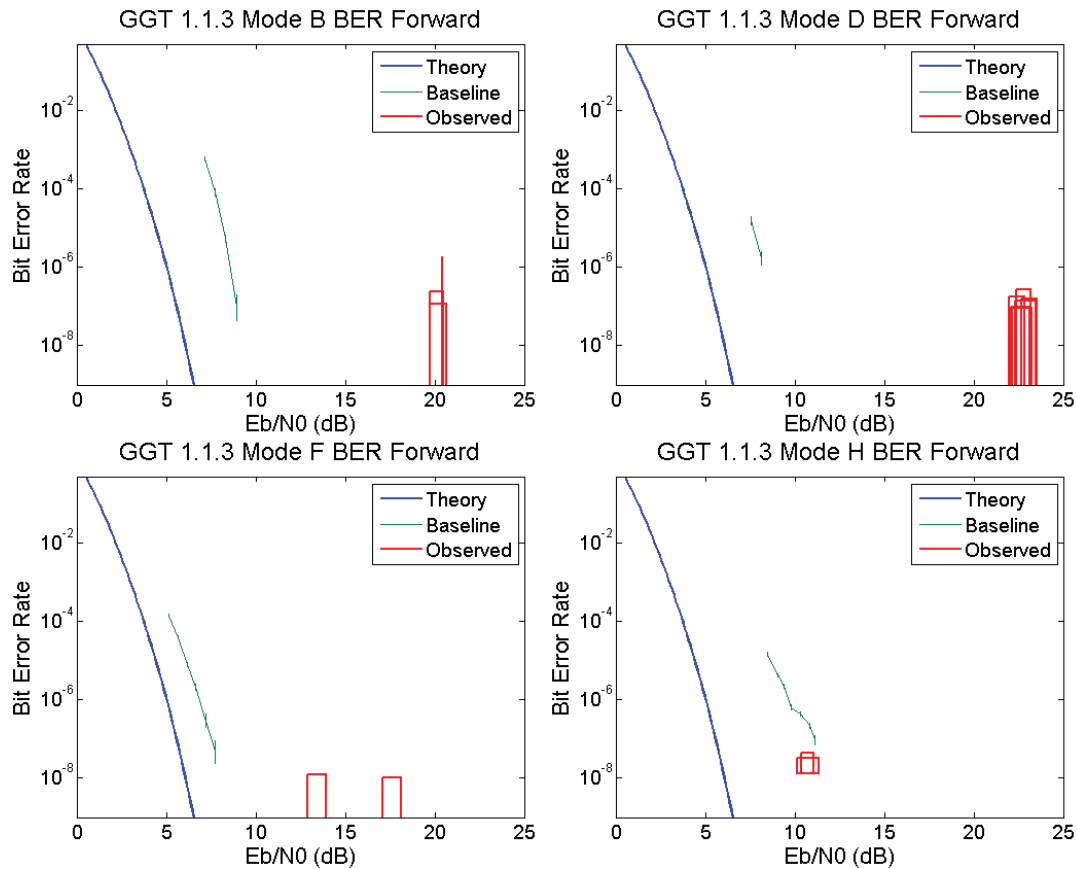


Figure 7.—GGT 1.1.3 Coded Forward Link BER Performance

Return Link Bit Error Rate Performance for Uncoded Modes

Unlike with the forward link measurements that use a predicted E_b/N_0 , the return link E_b/N_0 is measured by the integrated receiver (IR) at the White Sands Complex, which is the primary ground station for TDRSS. This value is translated to a signal-to-noise-density ratio (C/N_0) in data automatically returned by the Space Network Access System (SNAS) during an event. Empirical testing has shown that the SNAS C/N_0 is artificially higher than the equivalent IR E_b/N_0 ; unfortunately, the IR data is not returned routinely during or after a test.

To establish a usable E_b/N_0 , the SNAS C/N_0 is adjusted based on prior observed deviations between the IR E_b/N_0 and the calculated SNAS E_b/N_0 . The initial results show that the adjustment is based on data rate and coding, although there may be other factors that are not yet known. As a result of this uncertainty, the return link E_b/N_0 could have 2 to 3 dB error.

The uncoded return link performance is shown in Figure 8. The baseline performance was found during ground testing using a RT Logic TDRS Simulator (TSIM), which supports the various S-band TDRSS modes of operation. The implementation loss of the TSIM may be different than the implementation loss of the integrated receiver, meaning that the ground test results may be better or worse than the IR performance.

Testing in modes A, E, and G was completed using the medium-gain antenna (MGA), leading to a smaller variation in E_b/N_0 over each pass. The mode A tests had no observed errors, and the mode E tests generally were consistent with TSIM performance. The mode G tests show performance that is better than theory, which indicates that the E_b/N_0 for this particular mode is being estimated too low in the C/N_0 to E_b/N_0 conversion process by approximately 2 to 3 dB. Further calibration of the SNAS data is required.

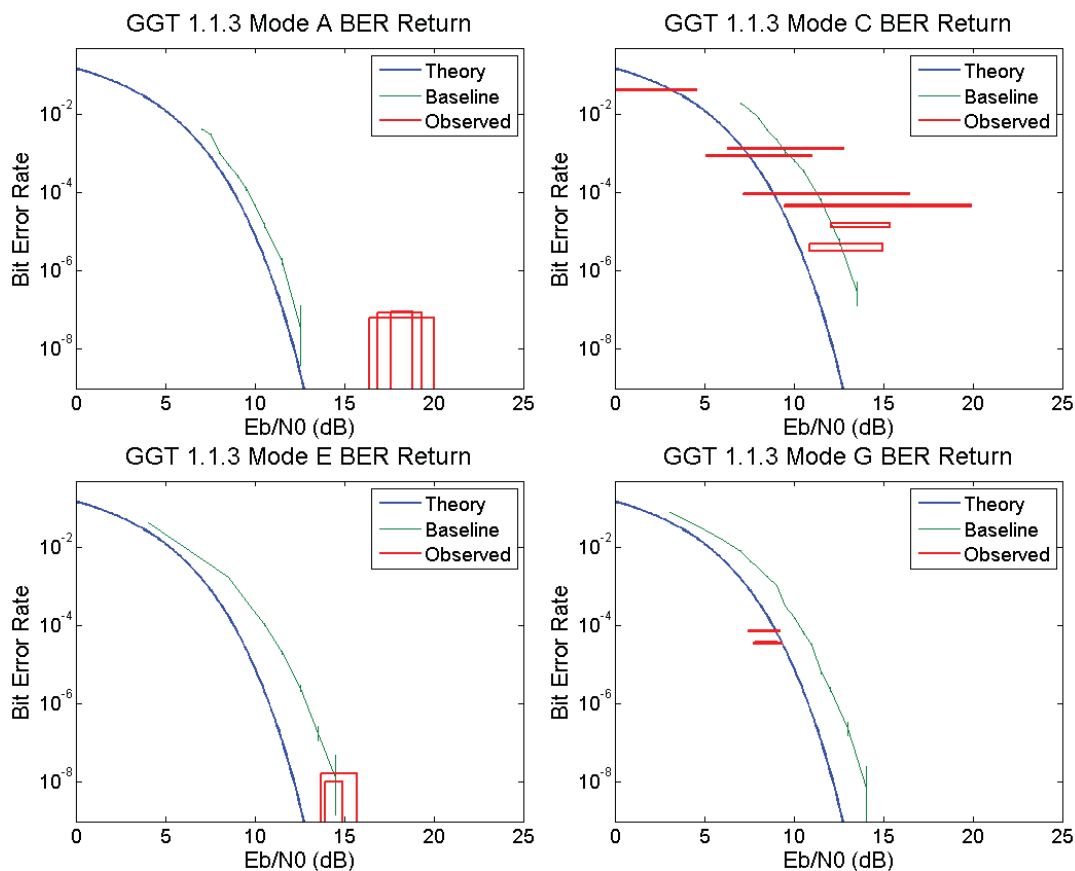


Figure 8.—GGT 1.1.3 Uncoded Return Link BER Performance

Testing in mode C was completed using the Space Network low-gain antenna (SN-LGA), which is less directional and results in a much wider variation in E_b/N_0 over a given pass. However, there is also less power received, which makes the BER simultaneously worse and much more certain. The tradeoff with using the MGA for this testing is that mode C likely would not have any observed errors. In the future, testing could be completed by reducing the radio transmit power and using the MGA to establish a tighter BER point.

Return Link Bit Error Rate Performance for Coded Modes

The GGT 1.1.3 waveform supports 4 coded transmit modes: B, D, F, and H. Each mode applies rate-1/2 convolutional coding to the transmit symbols. The ground receiver uses a Viterbi decoder to recover the data bits.

Waveform performance for the coded return link is shown in Figure 9.

As with the coded forward link modes, the coded return link performance is difficult to measure since it is unusual to have bit errors with such a short RF event. Mode B was not tested (performance would be similar to mode D). Both modes D and F ran a number of tests that completed without any observed errors. Mode H, due to its high data rate, was able to establish a characteristic BER. The performance here is within the realm of possibility: worse than theory but better than the TSIM baseline. Assuming the TSIM performance is very close to IR performance, the mode H E_b/N_0 estimate is low by 2 to 3 dB, similar to mode G above.

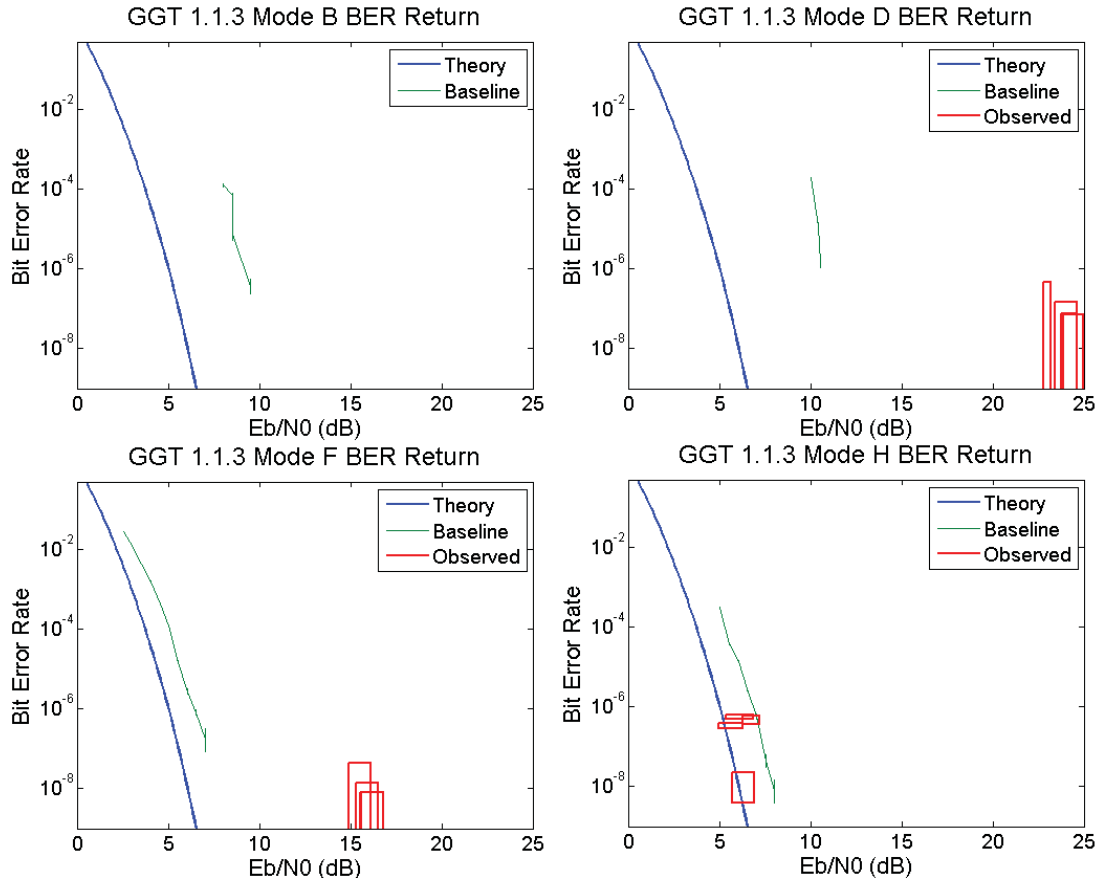


Figure 9.—GGT 1.1.3 Coded Return Link BER Performance

Forward Link Frequency Prediction

GGT provides a telemetry value for the forward link Costas loop frequency offset. The JPL radio contains a temperature-compensated crystal oscillator (TCXO) that varies over temperature. Figure 10 shows the oscillator drift at the SA transmit frequency, 2216.5 MHz, measured during thermal-vacuum (TVAC) testing. The frequency varies from about +200 Hz to +1200 Hz. During TVAC, one compensation table was developed and verified to offset the baseband frequency. Following additional data analysis, the table was revised to provide a more accurate correction shown by the lowest curve in green.

Since the same TCXO is used for both transmit and receive operations, the frequency offset in Figure 10 provides insight into the accuracy of the received frequency measurement. The TCXO cannot be compensated perfectly because it displays some hysteresis (for example, around 35 °C in the figure). Fortunately, the SNUG allows ± 700 Hz variation on the transmit frequency, which corresponds to a similar ± 700 Hz variation in the receive frequency accuracy.

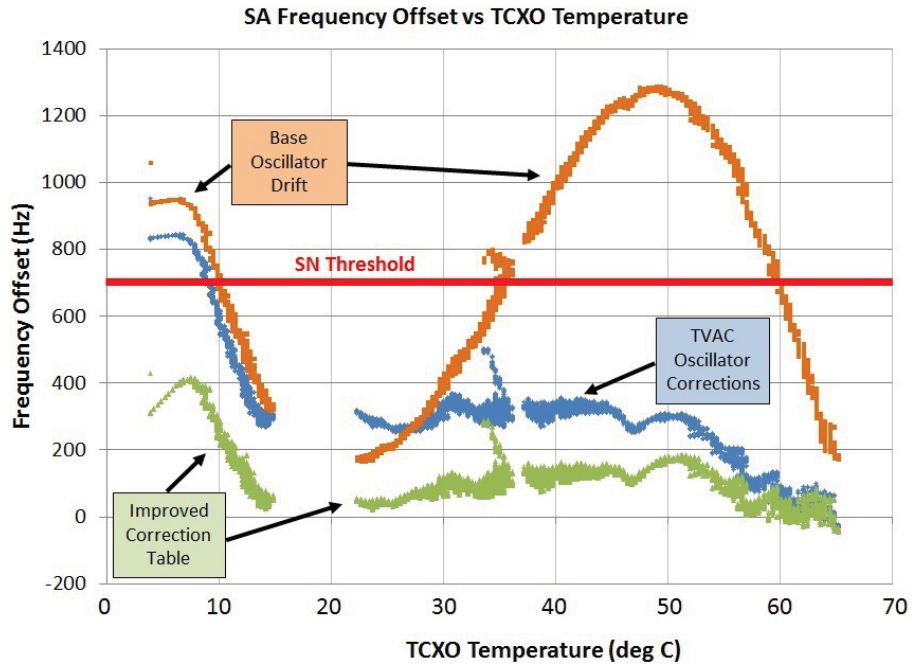


Figure 10.—JPL SDR TCXO Frequency Drift Over Temperature

For more information on the radio temperature compensation, please refer to SCan Testbed project document GRC-CONN-ANA-0855 (“Analysis of JPL FM SDR Temperature Compensation”).

The GGT waveform carrier recovery process determines the frequency offset of the received signal relative to the local oscillator expected frequency. That is, the local oscillator is programmed to 2041.027083 MHz for a SA signal and the oscillator offset required to match the center frequency of the received signal is provided in telemetry.

It would be incomplete to discuss the performance of the GGT waveform frequency accuracy without first mentioning the performance of the Space Network. In general, TDRSS applies Doppler compensation on the forward link so that the received frequency at the radio should be close to the intended center frequency. The TDRSS broadcast frequency is reported to the nearest 10 Hz and the expected broadcast frequency can be found using a STK model. For the tests in this report, TDRSS tends to transmit on average 150 Hz lower than expected.

The maximum, minimum, and average observed forward frequency offset applied by the GGT waveform is shown in Figure 11. These values are corrected for any frequency error introduced by the SN Doppler compensation.

On average the radio provides about 360 Hz more compensation than expected, which indicates that the JPL SDR oscillator is tuned about 360 Hz lower than the oscillator in TDRS. A negative value in the chart indicates that the waveform is increasing the frequency above expected, and a positive value indicates a lower frequency. What this means is that the oscillator compensation table may need adjusting on orbit to better reflect the TCXO performance over temperature. However, it is notable that all averages are within the ± 700 Hz acceptable range, which indicates the TCXO is in general performing similar to ground testing.

The maximum and minimum frequency offset is also shown for reference; however the values are less meaningful. The Costas loop bandwidth increases as the waveform symbol rate increases, so the frequency becomes harder to estimate in a high rate mode. An extreme frequency offset more likely implies inaccuracy in the Costas loop estimate and not TCXO error.

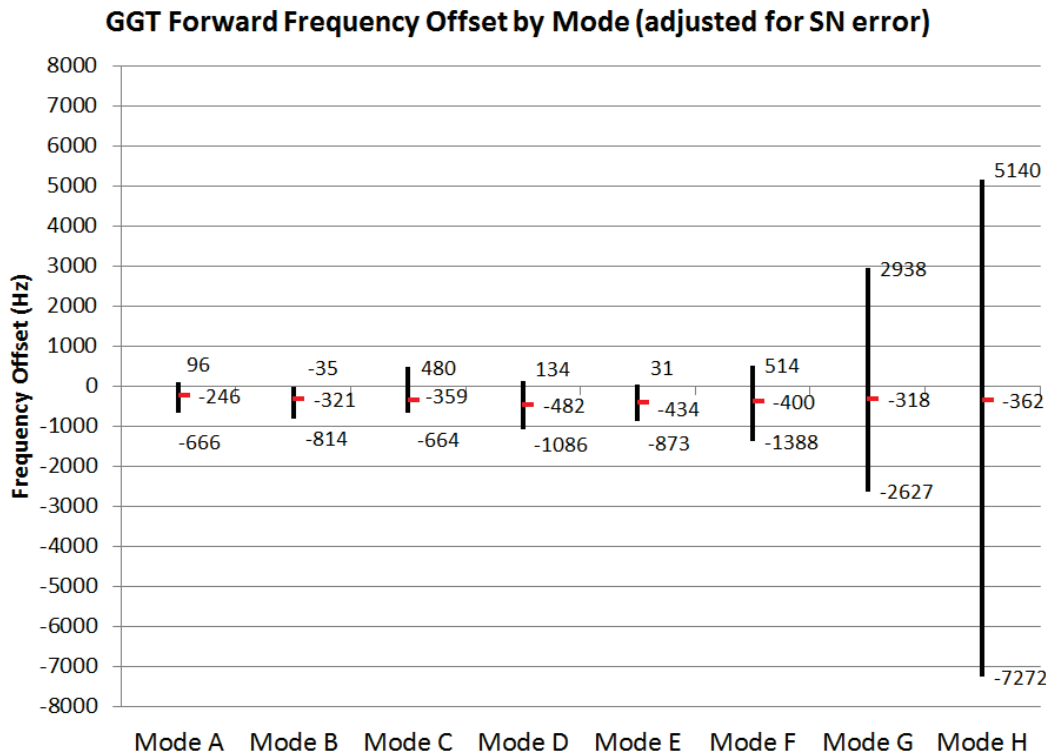


Figure 11.—GGT Forward Frequency Offset by Mode

The forward frequency offset is compared to temperature in Figure 12. A negative offset value indicates that the waveform frequency was too high—the frequency was increased too much. Therefore, the transmit frequency will also be too high and can be reduced by approximately 360 Hz on average.

Figure 12 does not show any trend over temperature. This is not surprising since the TCXO tends to be operated over a very narrow temperature band on-orbit, and the underlying TCXO does not have a significant trend over this range. The oscillator frequency varies more significantly (and exceeds +700 Hz) from 35 to 60 °C, which has not been seen outside of TVAC testing.

The figure shows that the temperature compensation tables could be updated with a DC offset. However, there is no significant trend in the data that would allow fine-tuning of the TCXO for the on-orbit conditions.

Forward Link Automatic Gain Control

The JPL SDR contains a series of gain stages that increase the received signal level (see JPL document D-49240, “CoNNeCT JPL-SDR FM HDD” for more information). The gain level is programmable in software and GGT implements a control algorithm in the FPGA. The algorithm adjusts the AGC gain until the wideband power at the analog-to-digital converter (ADC) is approximately 25 percent full scale.

The AGC level is programmable by digital number (DN). A lower DN provides higher gain, and a higher DN provides less gain. For example, DN 60 would amplify more than 120. In practice, the AGC level is limited by noise. During ground testing, the AGC reached a floor at digital number (DN) 85 for signals lower than approximately -110 dBm.

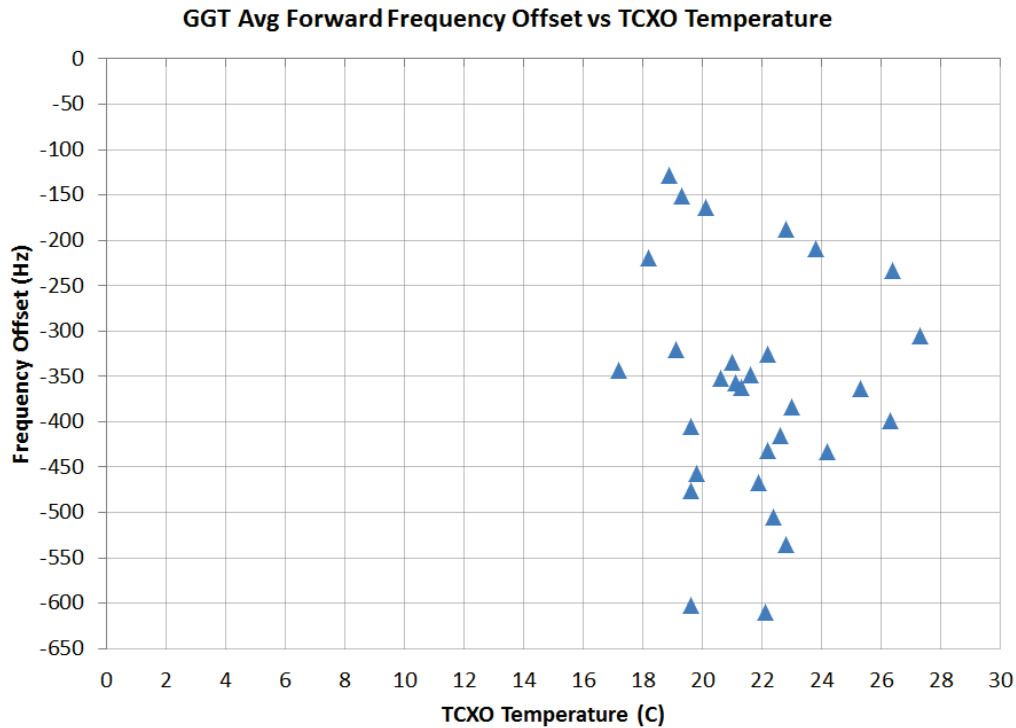


Figure 12.—GGT Forward Frequency Offset Versus TCXO Temperature

Roughly speaking, each DN represents about 0.5 dB of gain. For example, a change in the AGC value from 85 to 105 implies that the signal has become 10 dB stronger and therefore needs 10 dB less amplification. The exact AGC performance measured during TVAC is documented thoroughly in SCaN Testbed project document GRC-CONN-ANA-0854, “Analysis of JPL FM SDR Receiver Noise Figure and Gain”.

Figure 13 shows the AGC ranges seen on-orbit by waveform mode. Note that modes G and H have been excluded because the AGC set point is slightly different to compensate for the BER flare. The chart is interesting because it shows that the lowest AGC value of 85 on the ground is in some cases the highest observed AGC value on orbit! The average change of 10 DN suggests that the noise floor on-orbit of the space-facing antennas is approximately 5 dB lower than the noise floor seen during ground testing.

Another way to look at the AGC measurements is to compare the AGC to input power. This comparison is shown in Figure 14, with a couple interesting observations. First, the on-orbit AGC range is significantly different than the one seen on the GIU for similar input power. This makes it more difficult to predict on-orbit performance by simply running a test on the GIU. Second, there is a large span (~4 DN) to each cluster of AGC points at a given power level on orbit. This implies that the radio could see a power variation of 2 dB, independent of the signal level transmitted by TDRSS. The variation could be due to a change in the noise floor or an unknown interferer.

One conclusion of this analysis is that it may be difficult to predict waveform received power on-orbit with better than 2 dB accuracy using the AGC. Assuming changes in the noise floor are causing the AGC variation—which is a safe assumption given the AGC=75 data point around -106 dBm—then the Eb/N0 could vary unpredictably.

Another more positive conclusion is that the AGC appears to be a slightly better indicator of input power on orbit than on the GIU. During ground testing, the AGC changed significantly only for input power greater than -100 dBm. On orbit, the AGC range extends to approximately -105 dBm or lower.

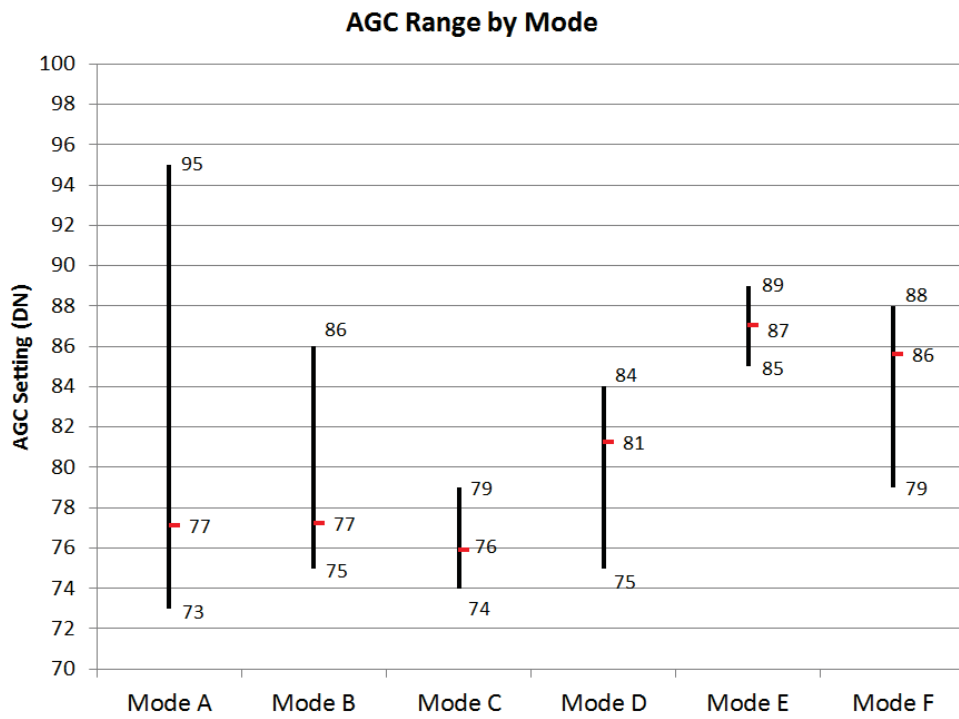


Figure 13.—AGC Range by Mode

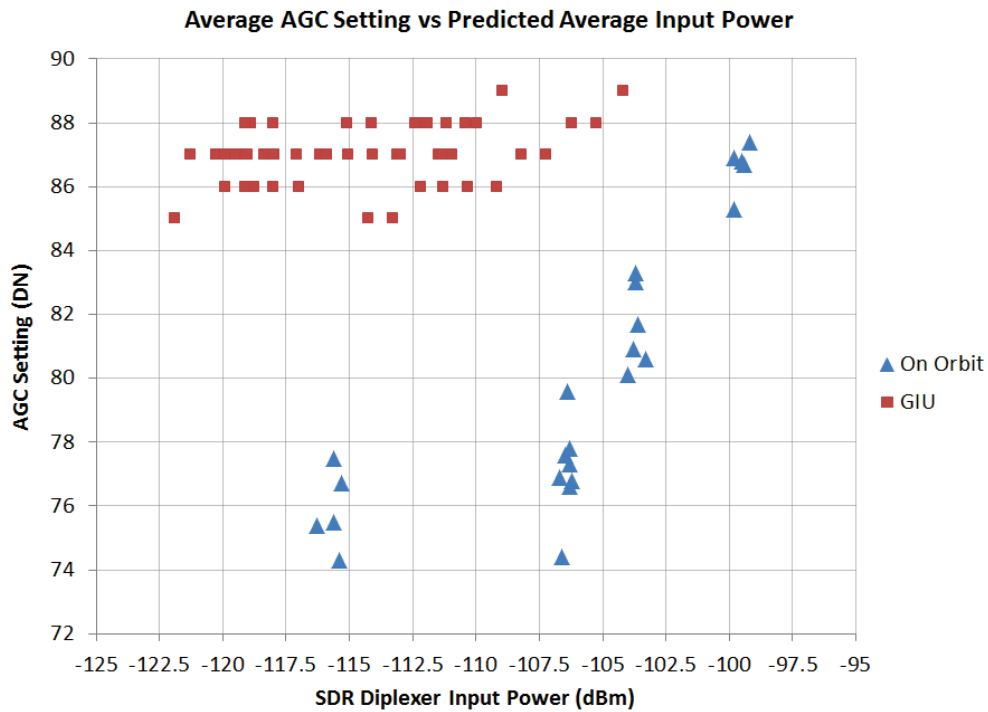


Figure 14.—Average AGC Setting vs Predicted Average Input Power

Characteristic Input Power Levels

The testing completed on GGT 1.1.3 tended to occur over certain specific combinations of payload antenna and TDRSS power level, as shown in Table 3. These combinations resulted in specific bins of input powers (such as in Figure 14) and a correspondingly limited range of E_b/N_0 values. Testing was limited to the TDRS satellites F8 and F10 to simplify link predictions. Grayed cells indicate that the test combination was not performed with GGT 1.1.3.

For each antenna, there is also a range of input powers that can be seen during a 40-min pass. These ranges are shown in Table 4. Note that the MGA antenna typically has a 1 dB variation throughout the pass, since it is steered by a gimbal assembly, while the SN-LGA antenna can vary by 5 dB.

TABLE 3.—AVERAGE POWER FOR TDRS TEST COMBINATIONS

	TDRS MA, F8-F10, dBm	TDRS SA, F8-F10 normal power, dBm	TDRS SA, F8-F10 high power, dBm
SN-MGA	-106.4	-103.7	-99.5 dBm
SN-LGA		-115.5	
NEN-LGA			

TABLE 4.—TYPICAL POWER RANGE FOR TDRS TEST COMBINATIONS

	TDRS MA, F8-F10, dBm	TDRS SA, F8-F10 normal power, dBm	TDRS SA, F8-F10 high power, dBm
SN-MGA	-106 ... -107	-103 ... -104	-99 ... -100
SN-LGA		-114 ... -119	
NEN-LGA			

The choice of antenna depends on the test objective. The MGA antenna is optimal for delivering stable power, but the SN-LGA antenna has far more varying link characteristics and can be used for acquisition threshold testing. There are some options for setting received power levels outside of the standard ranges:

1. The NEN-LGA can be used to communicate with a TDRS as it comes over the horizon. The initial power level is similar to the SN-LGA level, but the received power will decrease by about 20 dB over a 40-min pass.
2. The SN-MGA can be mispointed to reduce the received power by an arbitrary amount. This requires sufficient knowledge of the antenna pattern, but it has been demonstrated using the other radios in SCA_N Testbed.

For BER testing, the E_b/N_0 is determined by the data rate as well as the input power. Simply choosing a wider variation of data rates provides a substantial amount of E_b/N_0 possibilities.

Transmit Power Levels

TxRF Sensor

The JPL SDR contains a “TxRF” sensor, which is similar to a square law voltage detector on the transmit power out of the solid state power amplifier (SSPA). In general, the TxRF value increases as the RF output power of the radio increases. A detailed analysis of the sensor was conducted during TVAC,

and this is available in the SCaN Testbed project document GRC-CONN-ANA-0892, “Analysis of JPL SDR Flight Model Transmitter Characteristics”.

The GGT waveform includes an Automatic Level Control (ALC) algorithm that boosts the baseband power level by adjusting the I and Q drive levels to the digital-to-analog converter (DAC). The ALC uses an 8-point moving average on the TxRF value and then operates using closed-loop feedback to increase/decrease the baseband drive levels until the TxRF value enters a certain range.

The ALC target levels are programmed ahead of time and are specific to each mode. In general, these points are about 0.5 dB into compression on the SSPA. The ALC adjustment threshold is set to 15, meaning that the baseband power is modified until the TxRF value is within 15 DN of the target level. The settings for each waveform mode are shown in Table 5.

The observed on-orbit TxRF values are shown in Figure 15. Although the set points are not shown on the chart, all of the average values are within 3 DN of the desired target. The change in output power over the ranges is only about 0.3 dB on average despite the 100+ DN variation.

The TxRF values themselves do not indicate that the hardware is performing as expected. Since the ALC is a closed-loop algorithm, the drive level will increase until the TxRF sensor displays the correct value. The JPL SDR does not contain a redundant transmit power sensor, so the baseband drive level would simply be increased if the SSPA began to transmit at reduced capacity. Fortunately, this would eventually cause the DAC to clip, which would significantly increase the error vector magnitude (EVM) and result in a very poor BER.

TABLE 5 – ALC TARGETS AND THRESHOLDS

GGT Mode	TxRF Target, DN	Approx. Tx power, dBm	Adjustment threshold, DN
A	409	+37.5	15
B	409	+37.5	15
C	392	+37.6	15
D	392	+37.6	15
E	401	+37.5	15
F	401	+37.5	15
G	400	+37.4	15
H	400	+37.4	15

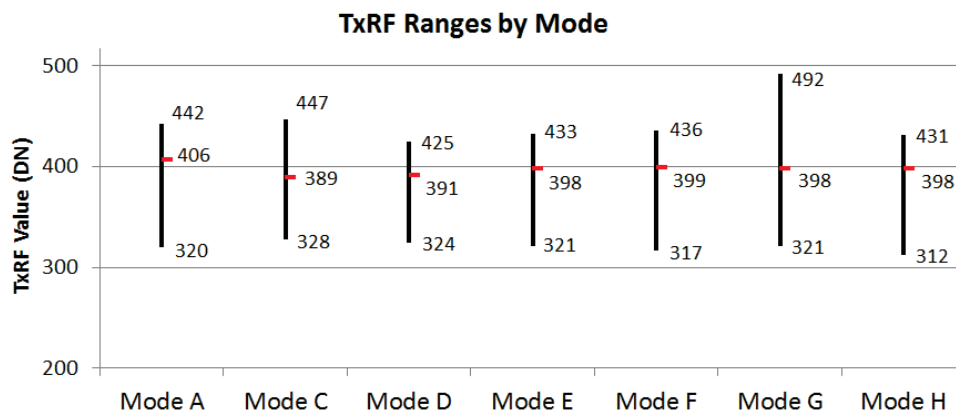


Figure 15.—TxRF Ranges

Return Link Carrier-to-Noise Density

Another check of the radio transmitter characteristics is the return link receiver C/N0 value. However, this is an indirect method. The S-band transmission of the JPL SDR is received by a TDRS transponder where it is shifted to Ku-band for the space-to-ground link. The signal is received by a dish at the White Sands Complex and routed to the integrated receiver (IR). The IR performs Eb/N0 estimation using a matched filter technique.

The Eb/N0 estimator is converted to a C/N0 value that is returned through SNAS. As previously mentioned, the conversion process appears to add a bias to the C/N0, which makes the C/N0 value higher than expected by 3 to 8 dB. The offset depends on data rate and coding.

SCaN Testbed is able to remove the SNAS C/N0 bias in post-processing. The IR Eb/N0s can be requested from White Sands after an event and compared to the SNAS C/N0s. After several coded and uncoded events at each data rate, a static offset was determined and removed from the SNAS values. However, it may take more events before the bias is better understood.

The return link C/N0 performance is shown in Figure 16 using the corrected SNAS C/N0.

Figure 16 shows that the return link performance for the GGT 1.1.3 events is generally close to the predicted performance. In the ideal case, all points would be on the 1:1 line through the center of the plot (i.e., the predicted C/N0 matches the measured C/N0). Modes A, D, E, and G match the ideal line. Mode C was tested using the SN-LGA antenna, so some variation can be expected due to the lower C/N0 and 5 dB power range over the pass. Mode F is consistently 1 to 2 dB better than expected and mode H is consistently 2 to 3 dB worse than expected. Since there is a minimal dataset for both of these modes, the performance can be attributed to an incorrect adjustment of the SNAS C/N0 value.

Another way of viewing C/N0 accuracy is to consider the return link BER in Figure 8 and Figure 9. The mode E BER matched TSIM performance, and here mode E is shown within 1 dB of the expected C/N0. Both mode G and mode H had a BER that seemed to indicate the Eb/N0 was low by 2 to 3 dB. The C/N0 results show that mode H appears to be lower than predicted by the same amount, which indicates the issue is C/N0 calibration and not a lower-performing link. However, mode G is very close to predicted, so more testing would be needed to improve prediction accuracy.

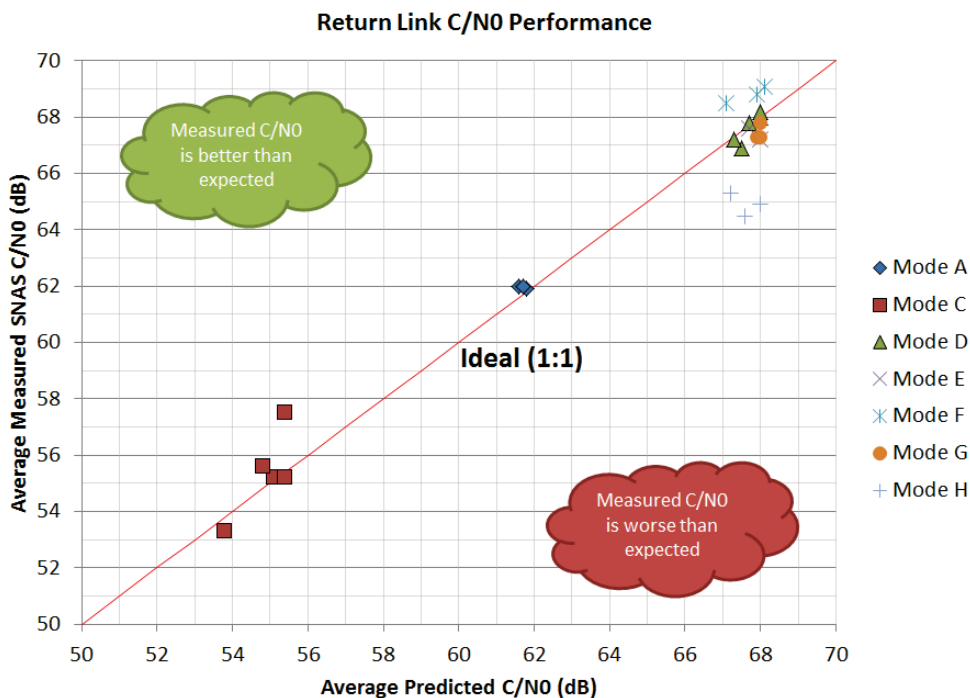


Figure 16.—Return Link C/N0 Results

Since the measured C/N0 values overall are close to predicted, it is reasonable to say that the SSPA is performing nominally. The return link C/N0, despite the bias, is a safer indicator of transmit power than the TxRF sensor since it is an independent measurement.

Future Work

Testing of GGT 1.1.3 is complete. GGT version 1.1.4 was released, and the new version includes a number of bug fixes and upgrades including:

- BER flare is resolved
- Soft-decision Viterbi is added
- Forward link power estimator is added
- Forward link signal-to-noise ratio estimator is added

Future testing will focus on verifying the GGT 1.1.4 bug fixes and new signal estimators.

Conclusions

This report has considered a number of the performance aspects of GGT 1.1.3, including bit error rate (summary in Table 6), frequency estimation, automatic gain control values, the TxRF sensor, and return link C/N0. In general, the performance of GGT meets expectations to within 2 to 3 dB of the predicted power levels across all modes of operation.

Future testing must focus on reducing measurement uncertainties. In particular, the variation in noise floor identified in this report points to the potential for in-band interference. The uncertainty in converting the SNAS C/N0 to a receiver Eb/N0 also must be reduced before more consistent performance can be attained.

TABLE 6.—SUMMARY OF TYPICAL BER PERFORMANCE FOR GGT 1.1.3

GGT mode	TDRS Tx power	SN-LGA		SN-MGA	
		Forward	Return	Forward	Return
A (MA)	Normal	-----	-----	1×10^{-7}	1×10^{-7}
B (MA)	Normal	-----	-----	1×10^{-7}	-----
C (SA)	High	-----	1×10^{-4}	-----	-----
	Normal	1×10^{-4}		-----	
D (SA)	High	-----	-----	-----	1×10^{-7}
	Normal	-----		1×10^{-7}	
E (SA)	High	-----	-----	2×10^{-7}	1×10^{-8}
	Normal	-----		-----	
F (SA)	High	-----	-----	1×10^{-8}	1×10^{-8}
	Normal	-----		-----	
G (SA)	High	-----	-----	1×10^{-5}	1×10^{-5}
	Normal	-----		-----	
H (SA)	High	-----	-----	1×10^{-8}	1×10^{-7}
	Normal	-----		-----	

